Published by:

The Electrochemical Society, Inc.
10 South Main Street
Pennington, New Jersey 08534-2896, USA

Telephone (609) 737-1902
Fax (609) 737-2743
e-mail: ecs@electrochem.org
Web site: http://www.electrochem.org

ISBN 1-56677-205-2

Printed in the United States of America

PROCEEDINGS OF THE ELEVENTH INTERNATIONAL SYMPOSIUM ON

MOLTON SALTS XI

Editors

P. C. Trulove
United States Naval Academy
Annapolis, MD

H. C. De Long
Air Force Office of Scientific Research
Bolling AFB, DC

G. R. Stafford
National Institute of Standards and Technology
Gaithersburg, MD

S. Deki
Kobe University
Kobe, Japan

PHYSICAL ELECTROCHEMISTRY, HIGH TEMPERATURE MATERIALS, AND ELECTRODEPOSITION DIVISIONS

Proceedings Volume 98-11

THE ELECTROCHEMICAL SOCIETY, INC.,
10 South Main St., Pennington, NJ 08534-2896, USA

THE REACTION BETWEEN MoO_3 AND MOLTEN $K_2S_2O_7$ FORMING $K_2MoO_2(SO_4)_2$, STUDIED BY RAMAN AND IR SPECTROSCOPY AND X-RAY CRYSTAL STRUCTURE DETERMINATION

T. Noerbygaard, R. W. Berg*, and K. Nielsen,
Department of Chemistry, DTU Building 207, Technical University of Denmark, DK-2800 Lyngby, Denmark

The reaction between molybdenum trioxide and molten potassium pyrosulfate was shown by Raman spectroscopy at 430 °C to be a 1:1 reaction. By tempering of the compound, colorless crystals could be formed. The structure was determined; crystal data: Space group = $P2_1/c$, $Z = 4$, a = 9.0144(3), b = 12.4540(4), c = 8.8874(3) Å, β = 112.194(1)°, wR_2 = 0.0897 for 3491 independent reflections. The compound, $K_2MoO_2(SO_4)_2$, contains MoO_2^{2+} core ions in distorted octahedral coordination, with two short (~1.69 Å) terminal bonds in *cis*-configuration (the O-Mo-O angle is 103.1(2)°), and with two long (~2.18 Å) bonds in *trans*-position to the short ones, and with two bonds of intermediate (~2.01 Å) length, all *four* bridging oxygens belonging to different sulfato groups. The K^+ ions are placed in between strands of MoO_6 octahedra, connected along the *c*-axis by two different kinds of bridging sulfato groups. Bond distances and angles are compared with literature values. Empirical correlations between bond distances and bond orders and bond order sums (approximating oxidation states) are given for all atoms. IR and Raman spectra were obtained and tentatively assigned.

* To whom correspondence should be sent (e-mail address: rwb@kemi.dtu.dk).

INTRODUCTION

The present work is part of a general study on metal ore extraction by pyrosulfate melting processes. We here report on the formation and structure of crystals, which were prepared by dissolving molybdenum trioxide in molten potassium pyrosulfate at 430 °C.

It is known that the relatively inert solid molybdenum trioxide (MoO_3) can be dissolved in hot disulfuric acid ($H_2S_2O_7$, oleum), in hydrogen fluoride acid (HF) and in various fused salts, *e.g.* alkali hydroxides, carbonates and pyrosulfates. Few modern studies have been performed on the behavior of MoO_3 in these systems. The type of compound formed by the dissolution of molybdenum trioxide in the pure pyrosulfate melt is unknown. Mo(VI) is expected to be able to form anionic sulfato complexes, and compounds like $MoO_2(HSO_4)_2$ and $Mo(HSO_4)_6$ have been proposed (1).

We therefore decided to mix MoO_3 and $K_2S_2O_7$ in varying molar amounts in sealed ampoules, which were heated to equilibration at 430 °C. The Raman spectra were recorded in an attempt to characterize any product which might be formed. From the results, we hoped by a method described in detail elsewhere (2), to be able to determine the reaction stoichiometry, and to isolate crystals suited for structure determination.

EXPERIMENTAL

Chemicals

The chemicals are hygroscopic and were therefore handled in an air-filled dry box. Anhydrous $K_2S_2O_7$ was synthesized by thermal decomposition of $K_2S_2O_8$ (Merck, p.a.) at 250 °C during 1 hour (3). Weighed amounts of $K_2S_2O_7$ and MoO_3 (Merck, 99%) were introduced into Pyrex cylindrical ampoules which were subsequently sealed under vacuum. The relative molar compositions are given in Table 1. When heated in a rocking furnace at 430 °C, all MoO_3 dissolved/reacted with the $K_2S_2O_7$, forming viscous yellowish melts. When cooled slowly, the melts froze forming microcrystalline lumps or (for higher Mo contents) clear glasses. When equimolar amounts of $K_2S_2O_7$ and MoO_3 (Merck, 99%) were taken into the ampoule, a clear glass of brutto formula $K_2MoS_2O_{10}$ resulted. No chemical analysis was made, since the composition of the melt was known, no attack on the Pyrex was seen, and the solidified mass looked homogeneous under a microscope. Crystals were grown by reheating this glass until start of crystallization at 280 °C and then by slowly cooling from that temperature in steps of 0.1 °C at a rate of 6 °C per hour. The ampoule was broken in the box and crystals taken out. The resulting crystals proved to be relatively stable in ambient air, but becoming bluish after some time, faster for small crystals. Melting of the crystals started above 405 °C, when seen under a microscope; some crystals remained until at least 411 °C.

Vibrational Spectra

Raman spectra were obtained by use of a DILOR XY 800 mm focal length multichannel spectrometer with macro and micro entrance, Ar-ion laser excitation (514.5 nm, 400 mW, vertically polarized), and CCD detection. Filtration of Rayleigh scattering was done with a Kaiser holographic SuperNotch-Plus filter or with a double *pre*-monochromator. The Raman spectral resolution was within 10 to 2 cm^{-1}. Temperature control was achieved by means of a home-made furnace or, for the case of crystals under the microscope, by a LINKAM HFS91/TP93 cryostat/furnace stage. A sheet analyzer, permitting vertically or horizontally polarized light to pass, was used to obtain polarization data.

The infrared absorption spectrum was obtained from a polycrystalline sample in KBr disk, measured against a KBr reference at room temperature on a Perkin-Elmer 1000 FT instrument (10 scans). The IR spectral resolution was ~4 cm^{-1}.

X-ray Diffraction

X-ray diffraction data were collected at 21 °C on a Siemens SMART diffractometer (4) using monochromated Mo-K_α (λ = 0.71073 Å) radiation. Unit cell dimensions were refined and intensity data were reduced (corrected for Lorentz and polarization effects) by use of the Siemens SAINT program system (4). The structure was solved by direct methods (5) and refined by full-matrix least-squares fitting of positional and anisotropic thermal parameters (6). Atomic scattering factors of Sheldrick (5) were used. Anomalous dispersion corrections were made by use of the Siemens SHELXTL program (5). Correction for absorption was done by means of the SADABS program (Siemens).

Crystal data and *R*-values are given in Table 2. Positional and equivalent isotropic thermal parameters are listed in Table 3, bond lengths and bond angles in Table 4. The packing of the structure is shown in Fig. 4, and the unit cell given in stereo in Fig. 5. Lists of observed and calculated structure factors and atomic anisotropic thermal parameters can be obtained from the authors.

RESULTS

Raman determination of stoichiometry

Raman spectra of melts at 430 °C as a function of the mole ratio, $\mathbf{X^0}(MoO_3)$, between MoO_3 and $K_2S_2O_7$ are shown in Fig. 1. The characteristic bands of $K_2S_2O_7$ (3) (top, $\mathbf{X^0}(MoO_3) = 0$) gradually disappear as the molybdenum mole ratio increases. At the same time, new bands appear monotonically, indicating that one and only one reaction has occurred. *E. g.*, it is seen that the 1085 cm^{-1} band of $K_2S_2O_7$ disappears and the new 958 cm^{-1} band of the mixture (new compound) increases with $\mathbf{X^0}(MoO_3)$. The integrated intensity ratio between these two bands above the background, I(Compound, 958 cm^{-1})/I($K_2S_2O_7$, 1085 cm^{-1}), is shown for each melt composition in Table 1.

The stoichiometry of the reaction could be determined from these results, by methods described in detail elsewhere (2). For the following analysis it is convenient to define the intensity ratios I* and I^O :

$$I^* = \frac{I(K_2S_2O_7, 1085\,cm^{-1})/\mathbf{X^0}(K_2S_2O_7)}{I(\text{Compound}, 958\,cm^{-1})/\mathbf{X^0}(MoO_3)} \qquad \text{[eq. 1]}$$

and

$$I^{O} = \frac{I(K_2S_2O_7, 1085\ cm^{-1}) / N_{eq}(K_2S_2O_7)}{I(Compound, 958\ cm^{-1}) / N_{eq}(Compound)} \qquad [eq.\ 2]$$

$N_{eq}(K_2S_2O_7)$ and N_{eq}(Compound) are the actual number of moles of $K_2S_2O_7$ and the new compound, respectively, present in the scattering volumne. N_{eq}(Compound) can only be calculated after assuming a value of the stoichiometric coefficient n in the reaction :

$$MoO_3 + n\,K_2S_2O_7 \Rightarrow Compound \qquad [eq.\ 3]$$

I* is plotted versus $\mathbf{X}(MoO_3)$ in Fig. 2. As seen, I* extrapolates to 0.55, indicating that all the $K_2S_2O_7$ has reacted at that composition. This points to a stoichiometry near 1:1 (n = 1). For a detailed discussion of the problems of determinating n from this kind of plot we refer to reference (2).

I^{O} is plotted versus $\mathbf{X}(MoO_3)$ in Fig. 3, for different assumed values of n. The numerator and denominator of equation 2 should each be *independent* on $\mathbf{X}(MoO_3)$; the scattering power *per* molecule of $K_2S_2O_7$ (numerator) or MoO_3 (denominator) should be universal *constants*, apart from an instrumental factor which cancels in equation 2. From Fig. 3 we conclude that the assumption of n =1 seems to be the most correct one. Thus we arrived at a product formula of $K_2MoS_2O_{10}$.

Table 1. Relative Raman scattering observed in the MoO_3-$K_2(S_2O_7)_2$ system as a function of Composition Mole Ratio.[a]

$X^0(MoO_3)$	$\frac{I(Compound, 958\ cm^{-1})}{I(K_2S_2O_7, 1085\ cm^{-1})}$	I*	I^{O} (n=1)
0.6823	saturated	-	-
0.5000	28.632	0.035	228.8
0.4003	2.8139	0.237	0.713
0.3334	1.7525	0.285	0.571
0.2498	0.7716	0.432	0.647
0.2004	0.5248	0.478	0.637
0.1670	0.3474	0.577	0.722
0.1506	0.2937	0.604	0.734
0.1183	0.2393	0.561	0.648
0.0995	0.1677	0.659	0.741
0.0918	0.1769	0.571	0.636
0.0632	0.1016	0.664	0.713
0.0479	0.0741	0.679	0.715

[a] For the meaning of symbols see the text.

X-ray structure

The X-ray crystal structure was solved in the monoclinic space group $P2_1/c$ (Table 2), showing that the crystals were indeed $K_2MoO_2(SO_4)_2$. The structure consists of potassium ions placed in between strands of MoO_6 octahedra, connected by bridging sulfato groups. The strands are parallel to the *c*-axis (Fig. 4). Each molybdenum atom is coordinated (at a distance of ~1.69 Å) to *two* terminal oxygen atoms in *cis*-coordination (the O-Mo-O angle is 103.1(2)°), and to *four* bridging oxygen atoms (with Mo-O bonds ~2.1 Å). [In the commonly found *cis*-arrangement the electronic repulsions are minimal because the oxygen p-electrons can use different empty molybdenum orbitals]. The Mo-O distances and O-Mo-O angle in MoO_2^{2+} core compounds are commonly found around 1.69(1)Å and 105(1)°, see (24). The four bridging oxygen atoms around Mo (O1, O2, O7, O8) are shared with four different sulfato groups. Each SO_4^{2-} group is coordinated [through *two* bridging oxygen atoms] to different molybdenum atoms (S-O bonds ~1.51 Å), the other *two* sulfato oxygen atoms being non-coordinated and having short S-O distances, ~1.435 Å. The Mo-O bonds experience a structural *trans*-influence, attributable to the competition among the O atoms along a shared axis (O3=Mo--O1 and O6=Mo--O2) for the σ and π orbitals of Mo. The O-Mo-O, O-S-O and Mo-O-S bond angles are in ranges 73-103°, 106-114° and 129-139°, respectively (Table 4). The considerable deviation of the O-Mo-O angles from 90° (O2-Mo-O1 is only 73.04°) shows that the distortion of the octahedral symmetry is considerable. The Mo-O1-S1, Mo-O2-S2, Mo-O7-S1 and Mo-O8-S2 bond angles are 137.0°, 132.1°, 128.8° and 138.9°, respectively. The shortest K-O contact distance is ~2.6 Å (K1-O5), see Table 4. No other crystal structure of molybdenum(VI) with sulfato coordination has been reported.

Bond length bond strength correlations

The obtained bond distances were used to determine bond orders by the method of correlation. Based on crystal structure data on many compounds, Brown and others (8)-(12) have developed general non-linear relationships between the atom-to-oxygen bond valence, *s*, and the atom-to-oxygen bond distance *R*. The empirical expression relating the *M*-O distance to the bond valency (*M* is an atom, here Mo, S or K) is

$$s(M\text{-O}) = s_o(R/R_1)^{-N} \qquad \text{[eq. 4]}$$

where s_o, R_1, and N are empirical constants. From the calculated values for the bond orders around any atom, the oxidation state of the atom can be estimated. In this way, the formal valence could be satisfactorily reproduced, see Table 5. Mo and S is in the +6

Table 2. Crystal Data for $K_2MoO_2(SO_4)_2$.

Formula	$K_2MoO_2(SO_4)_2$
M_w/g mol^{-1}	1593.04
Crystal size / mm	0.02*0.19*0.035
Crystal system	Monoclinic
V/Å^3	923.82(5)
Space group	$P2_1/c$
a/Å	9.0144(3)
b/Å	12.4540(4)
c/Å	8.8874(3)
β / °	112.194(1)
D_c/ g cm^{-3}	2.863
Temperature/K	293(2)
Z and F(000)	4 and 768
μ (Mo-K_α)/mm^{-1}	2.81
Extinction expression refined	$F_c^*=kF_c[1+0.001F_c^2\lambda^3/\sin(2\theta)]^{-1/4}$
Total no. of reflections	14470 (3491 independent)
Reflections collected	$-12 \le h \le 14$; $-18 \le k \le 19$; $-13 \le l \le 13$; $2.44 \le \theta \le 33.95$
Merging R factor	0.0547 ($\sigma^*(I)/I = 0.0612$)
Reflections with $I > 2\sigma(I)$	2518
No. of parameters	137
$R_1=\sum \lvert \lvert F_o \rvert - \lvert F_c \rvert \rvert / \sum \lvert F_o \rvert$	0.0826 for all reflectionns
	0.0455 for reflections with $F_o > 2\sigma(F_o)$
$wR_2=[\sum w(\lvert F_o \rvert - \lvert F_c \rvert)^2/\sum w \lvert F_o \rvert^2]^{1/2}$	0.0897 for all reflections
	0.0767 for reflections with $F_o > 2\sigma(F_o)$
Weight function, where $P=(F_o^2+2F_c^2)/3$	$w^{-1} = \sigma^2(F_o^2) + (0.0293P)^2 + 1.2766\,P$
Goodness of fit	1.122 for all reflections
	1.137 for reflections with $F_o > 2\,\sigma(F_o)$
Residual charge density/ e$^-$ Å^{-3}	$-1.3 \pm 0.2 < \rho < 1.1 \pm 0.2$

oxidation state, and K and O is in +1 and -2 state, respectively. Our structural results thus fit into the gereral results given in the literature (8)-(12). Such a fit provides a *vice versa* test of the plausability of the method of bond order summation and the crystal structure solution; the sum should lie within 5 % of the formal oxidation state (8).

Table 3. Fractional coordinates and equivalent isotropic thermal parameters.

Atom	x/a	y/b	z/c	U_{eq}/Å$^{2\,a}$
Mo	0.22155(4)	0.16810(3)	0.34641(4)	0.01610(10)
S1	0.43285(12)	0.35798(8)	0.62827(13)	0.0159(2)
S2	-0.03630(13)	0.30082(10)	0.02673(13)	0.0190(2)
K1	0.67997(15)	0.12213(10)	0.7049(2)	0.0355(3)
K2	0.8037(2)	0.01497(11)	0.1986(2)	0.0409(3)
O1	0.3002(4)	0.3208(3)	0.4778(4)	0.0229(7)
O2	0.1130(4)	0.2959(3)	0.1749(4)	0.0220(6)
O3	0.1402(4)	0.0687(3)	0.2111(4)	0.0260(7)
O4	0.4237(4)	0.4730(3)	0.6381(4)	0.0257(7)
O5	0.5859(4)	0.3196(3)	0.6359(4)	0.0266(7)
O6	0.3320(4)	0.1008(3)	0.5175(4)	0.0310(8)
O7	0.4037(4)	0.1931(3)	0.2718(4)	0.0215(6)
O8	0.0175(4)	0.1887(4)	0.3852(4)	0.0308(9)
O9	-0.1302(5)	0.2052(4)	0.0030(5)	0.0482(12)
O10	-0.1220(5)	0.3974(4)	0.0306(5)	0.0472(12)

[a] U_{eq} is defined in e.g. ref. (19).

Mean angle-distance correlation in sulfato groups

In the two sulfato groups, the S-O′ distance, O′ being a bridging oxygen atom, is significantly longer than other (non-bridging) S-O distances, see Table 4. Also, the two angles, O5-S1-O4 and O9-S2-O10, among terminal sulfato O atoms are significantly larger (around 113.9-114°) than the ideal tetrahedral angle. In our laboratory, an approximately linear relationship has been found, between the average of the three O-S-O angles involving a particular bond between sulfur and oxygen (non-bridging as well as bridging) and the length of that S-O bond, for a number sulfato compounds of vanadium (13)-(21) (errors in average angles in (21) have been corrected). Around the sulfur atoms, nearly tetrahedral angles were found, however deformed in such a way that O-S-O angles involving an oxygen atom bridging to the metal were smaller than the ideal tetrahedral angle of 109.47°. This is believed to be due to repulsion from the short-bonded oxygens. The O-S-O angles not involving bridging oxygen atoms enlarged to values above 109.47°. The S-O distances were found to depend on the angles in such a way that the larger the average of the three possible O-S-O angles involving a particular bond, the smaller is the S-O distance. A plot of the relation is shown in Fig. 6, together with the 8 points which can be deduced from this work. Obviously, the new points relating to $K_2MoO_2(SO_4)_2$ fit very well with the previous vanadium results. The relation in Fig. 6 must be taken to indicate a general trend between bond distances and hybridization of the central atom in tetrahedral sulfur.

Table 4. Bond Distances Angles in the $K_2MoO_2(SO_4)_2$ Structure.

Distances (Å)		Angles (degrees)		Angles (degrees)	
Mo-O1	2.204(3)	O3-Mo-O6	103.1(2)	O8-Mo-O2	80.09(14)
Mo-O2	2.165(3)	O3-Mo-O8	92.1(2)	O7-Mo-O2	82.09(13)
Mo-O3	1.689(3)	O6-Mo-O8	100.1(2)	O3-Mo-O1	167.5(2)
Mo-O6	1.692(3)	O3-Mo-O7	93.86(15)	O6-Mo-O1	89.4(2)
Mo-O7	2.014(3)	O6-Mo-O7	95.5(2)	O8-Mo-O1	86.07(15)
Mo-O8	2.012(3)	O8-Mo-O7	161.6(2)	O7-Mo-O1	84.37(13)
		O3-Mo-O2	94.5(2)	O2-Mo-O1	73.04(13)
		O6-Mo-O2	162.4(2)		
S1-O1	1.491(3)	O5-S1-O4	113.9(2)	O5-S1-O7	106.6(2)
S1-O4	1.440(4)	O5-S1-O1	111.7(2)	O4-S1-O7	109.3(2)
S1-O5	1.437(3)	O4-S1-O1	108.6(2)	O1-S1-O7	106.6(2)
S1-O7	1.534(3)				
S2-O2	1.487(3)	O9-S2-O10	114.0(3)	O9-S2-O8	107.9(3)
S2-O9	1.430(4)	O9-S2-O2	112.6(2)	O10-S2-O8	106.9(3)
S2-O10	1.437(4)	O10-S2-O2	109.2(2)	O2-S2-O8	105.8(2)
S2-O8	1.515(3)				

Distances (Å)					
K1-O5	2.597(4)	K1-O4	2.693(4)	K1-O9	2.756(5)
K1-O10	2.781(5)	K1-O3	2.814(4)	K1-O6	2.956(4)
K1-O6	3.386(4)				
K2-O5	2.754(4)	K2-O1	2.842(4)	K2-O2	2.939(4)
K2-O8	2.955(4)	K2-O4	2.965(4)	K2-O10	2.975(5)
K2-O3	3.068(4)	K2-O9	3.126(5)	K2-O4	3.264(4)
K2-O10	3.310(5)				

Table 5. Empirical Bond Orders (s) and Bond Order Sums (Σs) in $K_2MoO_2(SO_4)_2$, based on Bond Distances R. $s = s_o(R/R_1)^{-N}$ (s_o, R_1 and N are literature parameters).

Bond	Bond Order $s^{a,b,c}$	Σs^d	Bond	Bond Order $s^{a,b,c}$	Σs^d
Mo-O1	0,388 ± 0,003		O1-Mo	0,388 ± 0,003	
Mo-O2	0,431 ± 0,004		O1-S1	1,402 ± 0,011	
Mo-O3	1,914 ± 0,020		O1-K2	0,123 ± 0,001	1,91 ± 0,02
Mo-O6	1,894 ± 0,020		O2-Mo	0,431 ± 0,004	
Mo-O7	0,666 ± 0,006		O2-S2	1,417 ± 0,012	
Mo-O8	0,670 ± 0,006	5,96 ± 0.06	O2-K2	0,104 ± 0,001	1,95 ± 0,02
S1-O1	1,402 ± 0,011		O3-Mo	1,914 ± 0,020	
S1-O4	1,611 ± 0,018		O3-K1	0,129 ± 0,001	
S1-O5	1,625 ± 0,013		O3-K2	0,084 ± 0,001	2,13 ± 0.02
S1-O7	1,251 ± 0,010	5,89 ± 0.05	O4-S1	1,611 ± 0,018	
S2-O2	1,417 ± 0,012		O4-K1	0,161 ± 0,001	
S2-O9	1,657 ± 0,018		O4-K2	0,100 ± 0,001	
S2-O10	1,625 ± 0,018		O4-K2	0,062 ± 0,001	1,93 ± 0,02
S2-O8	1,315 ± 0,011	6,01 ± 0.06	O5-S1	1,625 ± 0,013	
K1-O3	0,129 ± 0,001		O5-K1	0,193 ± 0,002	
K1-O4	0,161 ± 0,001		O5-K2	0,144 ± 0,001	1,96 ± 0,02
K1-O5	0,193 ± 0,002		O6-Mo	1,894 ± 0,020	
K1-O6	0,101 ± 0,001		O6-K1	0,101 ± 0,001	
K1-O6	0,051 ± 0,001		O6-K1	0,051 ± 0,001	2,05 ± 0.02
K1-O9	0,143 ± 0,001		O7-Mo	0,666 ± 0,006	
K1-O10	0,137 ± 0,001	0.92 ± 0.01	O7-S1	1,251 ± 0,010	1,92 ± 0,02
K2-O1	0,123 ± 0,001		O8-Mo	0,670 ± 0,006	
K2-O2	0,104 ± 0,001		O8-S2	1,315 ± 0,011	
K2-O3	0,084 ± 0,001		O8-K2	0,101 ± 0,001	2,09 ± 0,02
K2-O4	0,100 ± 0,001		O9-S2	1,657 ± 0,018	
K2-O4	0,062 ± 0,001		O9-K1	0,143 ± 0,001	
K2-O5	0,144 ± 0,001		O9-K2	0,076 ± 0,001	1,88 ± 0,02
K2-O8	0,101 ± 0,001		O10-S2	1,625 ± 0,018	
K2-O9	0,076 ± 0,001		O10-K1	0,137 ± 0,001	
K2-O10	0,098 ± 0,001		O10-K2	0,098 ± 0,001	
K2-O10	0,057 ± 0,001	0.95 ± 0.01	O10-K2	0,057 ± 0,001	1,92 ± 0,02

[a] For Mo^{6+}, the expression of Brown and Wu (11) was used: s = (R/1.882 Å) ^ -6.00. This expression was based on 50 selected crystal structure determinations. Rather similar values were obtained from expressions of Schröder (9), s = 10 ^{(1.874 Å -R)/0.600}, and Allmann (10), s = 10 ^ {(1.90 Å -R)/0.76}. [b] For S^{6+}, the expression of Brown and Shannon (8) was used: s = 1.5(R/1.466 Å) ^-4.00. Rather similar s values were obtained by using their 10-

electron cation core universal expression, s = (R/1.622 Å) ^ -4.290. [c] For K^+ the expression of Brown and Wu was used: s = (R /1.882 Å) ^ -6.00. Comparable s values were obtained with expressions of Schröder, s = 10 ^ {(1.874 Å -R)/ 0.600}, and Allmann, s = 10 ^{(1.90 Å -R)/ 0.76}. [d] The sum is an estimation of the oxidation state of the atom.

Vibrational spectra, expectations

The MoO_2^{2+} ion has three vibrational degrees of freedom, which under C_{2v} point group symmetry transform as $2A_1$ (ν_1 (sym.str.), ν_2 (bend.)) + B_2 (ν_3 (asym.str.)). These modes may all be observed in IR and Raman spectra (Table 6, left). The bands have been observed in many MoO_2^{2+} core compounds with distorted octahedral configuration. In general, ν_1 and ν_3 occur as strong bands in IR and Raman spectra at ~910-950 cm^{-1} (ν_1) and ~880-920 cm^{-1} (ν_3) (22)-(24). *E.g.*, in the *cis*-$[MoO_2(thiooxine)_2]$ complex with known distorded octahedral coordination, strong IR and Raman bands were seen near 920 cm^{-1} (ν_1) and 893 cm^{-1} (ν_3) (23). Also, in *cis*-$[MoO_2X_2(OPPh_3)_2]$ complexes (X = F, Cl, Br, Ph = phenyl), IR bands were seen near 945 cm^{-1} (ν_1), 910 cm^{-1} (ν_3), and 260 cm^{-1} (ν_2) (25). Therefore, we expect to observe MoO_2^{2+} bands at the following positions: $\nu_1 \cong$ 910-950, $\nu_3 \cong$ 880-920, and $\nu_2 \cong$ 260 cm^{-1}.

The internal vibrations of a regular SO_4^{2-} ion of T_d of symmetry span the representation $A_1(\nu_1) + E(\nu_2) + 2F_2(\nu_3+\nu_4)$. All symmetry species are Raman and F_2 ones are IR observable (Table 7, left). The modes labelled ν_1 and ν_3 are bond stretchings, and ν_2 and ν_4 are mostly angle bendings within the SO_4^{2-} tetrahedron. The positions of the fundamental bands are well known: $\nu_1 \cong 983$, $\nu_2 \cong 450$, $\nu_3 \cong 1105$ and $\nu_4 \cong 611$ cm^{-1} (26).

The 4 MoO_2^{2+} ions in the *primitive* unit cell perform vibrations, which are distributed on the symmetry species of the cell. Under C_{2h}^5 factor group symmetry they span the representation $3A_g + 3B_g + 3A_u + 3B_u$, of which the *gerade* species are Raman and the *ungerade* ones are IR permitted. Since the MoO_2^{2+} ions sit on sites of no symmetry, the normal modes will be evenly distributed over all the symmetry species, see the correlation diagram given in Table 6 (correlating the modes of the free ions to those of the ions bound in the crystal).

In a similar way the 8 SO_4^{2-} ions in the *primitive* unit cell *each* contribute 9 internal degrees of vibrational freedom (inherent in the T_d sulfate modes ν_1-ν_4). These are also distributed on the symmetry species of the cell, spanning internal vibrations under the representation $18A_g + 18B_g + 18A_u + 18B_u$ (distributed evenly over the symmetry types of the C_{2h}^5 factor group). Some of these modes are stretchings and some are mixtures of stretchings and bendings, see the correlation diagram given in Table 7 (correlating the sulfate modes from the free to the bound state).

Table 6. Correlation Diagram for the Internal Vibrations in the 4 MoO_2^{2+} ions in the Unit Cell of $K_2MoO_2(SO_4)_2$.[a]

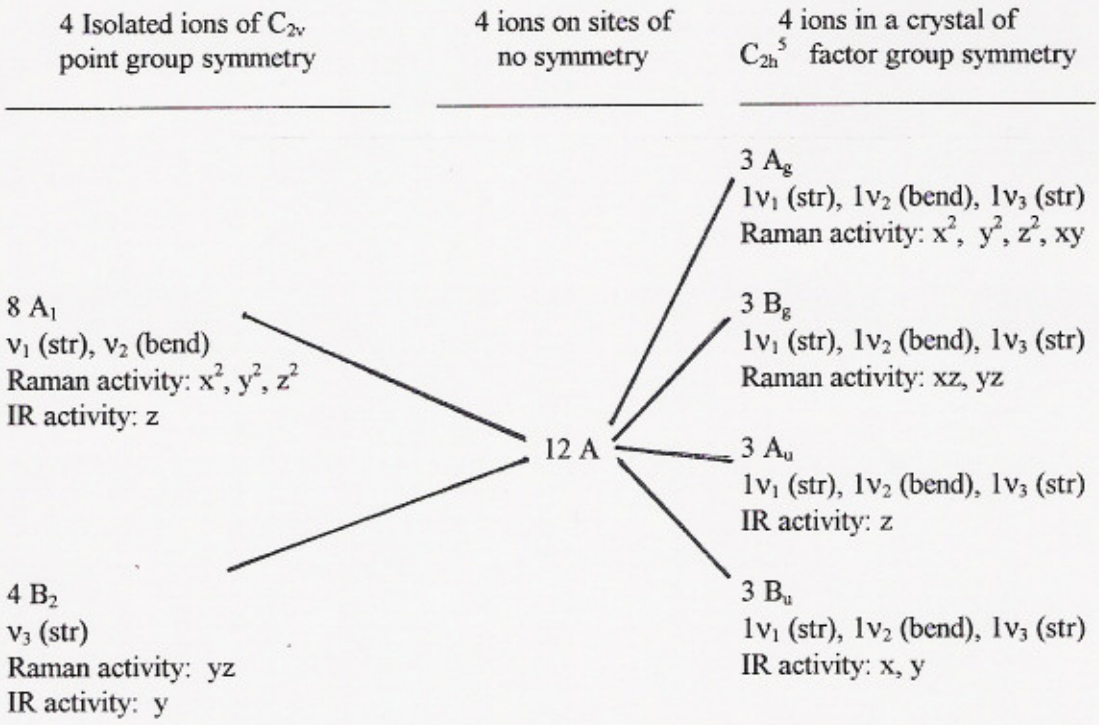

[a] Code: ν_1(str), ν_2(bend), and ν_3(str) are the $2A_1$ and B_2 stretching and bending modes of the MoO_2^{2+} group under C_{2v}-symmetry.

Many of the MoO_2^{2+} and SO_4^{2-} modes occur in same spectral range and with the same symmetry. Probably the Mo-O and the S-O stretchings are highly coupled. With the crystal structure known we can work out the complete selection rules based on the factor group analysis (27), (28) in the common wavevector $\mathbf{k} \cong 0$ approximation (Table 8). In total, for the crystal 90 Raman permitted fundamentals ($45A_g + 45B_g$) and 87 IR permitted fundamentals ($44A_u + 43\ B_u$) should be observable by use of suitably polarized light.

Interpretation of observed spectra

The observed Raman and IR spectra of the crystal at room temperature, and Raman spectra of the crystal at low or higher temparatures until melting are depicted in Figs. 7-8. Observed band positions and tentative assignments are given in Table 9. As can be seen, many bands are found in the spectra, but much fewer than predicted above; *e.g.* we observed about 38 bands in the Raman spectrum at low temperatures.

Table 7. Correlation Diagram for the Internal Vibrations in the 8 SO_4^{2-} ions in the Unit Cell of $K_2MoO_2(SO_4)_2$.[a]

8 Isolated ions of T_d point group symmetry	8 ions on sites of no symmetry	8 ions in a crystal of C_{2h}^5 factor group symmetry
		18 A_g $2\nu_1$ (str), $4\nu_2$ (bend), $6\nu_3$ (str), $6\nu_4$ (bend) Raman activity: x^2, y^2, z^2, xy
8 A_1 ν_1 (str) Raman activity: $x^2+y^2+z^2$		18 B_g $2\nu_1$ (str), $4\nu_2$ (bend), $6\nu_3$ (str), $6\nu_4$ (bend) Raman activity: xz, yz
8 E ν_2 (bend) Raman activity: $2z^2-x^2-y^2$, x^2-y^2	72 A	18 A_u $2\nu_1$ (str), $4\nu_2$ (bend), $6\nu_3$ (str), $6\nu_4$ (bend) IR activity: z
16 F_2 ν_3 (str), ν_4 (bend) Raman activity: xz, yz, xy IR activity: x, y, z		18 B_u $2\nu_1$ (str), $4\nu_2$ (bend), $6\nu_3$ (str), $6\nu_4$ (bend) IR activity: x, y

[a] Code: ν_1(str), ν_2(bend), ν_3(str), and ν_4(bend) are the A_1, E and $2F_2$ stretching and bending mode components of the SO_4^{2-} group under T_d-symmetry.

The bands have been tentatively interpreted as Mo-O and S-O stretchings and bendings, as indicated. The characteristic MoO_2^{2+} stretchings, expected at ~950 to ~880 cm^{-1}, we believe to see at 946, 931, 919 and 894 cm^{-1}. The characteristic SO_4^{2-} stretchings, expected at ~983 and ~1105 cm^{-1}, we assign to bands in the range 1294 to1007 cm^{-1}. The strongly polarized Raman band observed at 1026 cm^{-1} (25 °C) can hardly be assigned to anything else than $\nu_1(SO_4^{2-})$ even though this mode normally occurs at around 856-1002 cm^{-1}(26). The O-Mo-O deformation modes ν_2 , expected at ~260 cm^{-1}, probably are contained in bands at 279-394 cm^{-1}. In the sulfate bending range (~400-700 cm^{-1}) and in the lattice mode range (below ~400 cm^{-1}), the many observed bands are difficult to assign definitively, because extensive couplings of most of the normal modes are expected.

ACKNOWLEDGEMENTS

This work was supported by several Danish foundations which made purchase of the DILOR Raman instrument and its accessories possible: The Danish Technical Science Foundation, Corrit Foundation, Tuborg Brewery Foundation, Danfoss A/S, Thomas B. Thrige Foundation, P.A. Fiskers Foundation, Direktør Ib Henriksens Foundation. Also, we received help from Soghomon Boghosian, Rasmus Fehrmann and Niels J. Bjerrum.

REFERENCES

(1) A. Bali and K. C. Malhotra, *Aust. J. Chem.* **28**, 481 (1975).
(2) S. Boghosian, F. Borup and R. W. Berg, *In press* (This volume).
(3) N. H. Hansen, R. Fehrmann, and N. J. Bjerrum, *Inorg. Chem.* **21**, 744 (1982).
(4) Siemens SMART and SAINT. Data Collection and Processing Software for the SMART System, Siemens Analytical X-ray Instruments Inc., Madison, Wisconsin, USA (1995).
(5) G. M. Sheldrick, Program SHELXTL/PC Version 5.0. Siemens Analytical X-ray Instruments Inc., Madison, Wisconsin, USA (1994).
(6) G. M. Sheldrick, Program SHELXL97. Siemens Analytical X-ray Instruments Inc., Madison, Wisconsin, USA (1997).
(7) Bo Bergmann, CRYSTINFO, A CIF based crystallographic visualizer, University of Aarhus, Denmark (1995).
(8) I. D. Brown and R. D. Shannon, *Acta Cryst* **A29**, 266 (1973).
(9) F. A. Schröder, *Acta Cryst.* **B31**, 2294 (1975).
(10) R. Allmann, *Monatsh. Chem.* **106**, 779 (1975).
(11) I. D. Brown and K. K. Wu, *Acta Cryst* **B32**, 1957 (1976).
(12) J. C. J. Bart and V. Ragaini, *Inorg.Chim. Acta* **36**, 261 (1979).
(13) R. Fehrmann, B. Krebs, G. N. Papatheodorou, R. W. Berg and N. J. Bjerrum, *Inorg. Chem.* **25**, 1571 (1986).
(14) R. Fehrmann, S. Boghosian, G. N. Papatheodorou, K. Nielsen, R. W. Berg and N. J. Bjerrum, *Inorg. Chem.* **28**, 1847 (1989).
(15) R. Fehrmann, S. Boghosian, G. N. Papatheodorou, K. Nielsen, R. W. Berg and N. J. Bjerrum, *Inorg. Chem.* **29**, 3294 (1990).
(16) R. Fehrmann, S. Boghosian, G. N. Papatheodorou, K. Nielsen, R. W. Berg and N. J. Bjerrum, *Acta Chem. Scand.* **45**, 961 (1991).
(17) K. Nielsen, R. Fehrmann and K. M. Eriksen, *Inorg. Chem.* **32**, 4825 (1993).
(18) R. W. Berg, S. Boghosian, N. J. Bjerrum, R. Fehrmann, B. Krebs, N. Sträter, O. S. Mortensen and G. N. Papatheodorou, *Inorg. Chem.* **32**, 4714 (1993) and **33**, 402 (1994).
(19) S. Boghosian, R. Fehrmann and K. Nielsen, *Acta Chem. Scand.* **48**, 724 (1994).
(20) S. Boghosian, K. M. Eriksen, R. Fehrmann and K. Nielsen, *Acta Chem. Scand.* **49**, 703 (1995).

(21) K. M. Eriksen, K. Nielsen and R. Fehrmann, *Inorg. Chem.* **35**, 35 (1996).
(22) W. P. Griffith and T. D. Wickins, *J. Chem. Soc. A* **1968**, 400 (1968).
(23) L. J. Willis, T. M. Loehr, K. F. Miller, A. E. Bruce and E. I. Stiefel, *Inorg. Chem.* **25**, 4289 (1986).
(24) E. I. Stiefel, Molybdenum(VI), In "Comprehensive Coordination Chemistry", Vol. 3, Chpt. 36.5, p.1375, Sir G. Wilkinson, Editor-in-Chief, Pergamon Press (1987).
(25) R. J. Butcher, B. R. Penfold and E. Sinn, *J. C. S. Dalton Trans.* **1979**, 668 (1979).
(26) Nakamoto, K. *"Infrared and Raman Spectra of Inorganic and Coordination compounds"*, Wiley, New York, part A p. 189 and part B p. 79 (1997).
(27) D. L. Rousseau, R. P. Bauman and S. P. S. Porto, *J. Raman Spectrosc.* **10**, 253 (1981), and references cited there.
(28) D. M. Adams and D. C. Newton, *Tables for Factor Group and Point Group Analysis*, Beckman – RIIC Limited, England (1970).

Paper submitted on May 2, 1998.

Table 8. Factor Group Analysis[a] for the $K_2MoO_2(SO_4)_2$ Salt crystallizing in Space Group C_{2h}^5 ($P2_1/c$, No. 14, $Z = 4$).

	T_a	T	$R(SO_4^{2-})$	$R(MoO_2^{2+})$	$N_i(SO_4^{2-})$	$N_i(MoO_2^{2+})$	Activity in
<-------- Optically active normal modes -------->							
A_g	0	15	6	3	18	3	Raman: x^2, y^2, z^2, xy
B_g	0	15	6	3	18	3	Raman : xy, yz
A_u	1	14	6	3	18	3	IR : z
B_u	2	13	6	3	18	3	IR: x, y
Total	3	57	24	12	72	12	180 degrees of freedom

[a] The *primitive* unit cell contains 4 formula units of 15 atoms each, i.e. a total of 60 atoms. The T and R classification is based on the same cell considered as containing the following 20 ions: 8 K^+ ions, 4 MoO_2^{2+} ions and 8 SO_4^{2-} ions, all on Wyckoff site *e* with no site symmetry. T_a = optically inactive acoustic modes, T = optic branch translatory modes of the 20 ions, ($T + T_a$ = 3 times 20), $R(SO_4^{2-})$ and $R(MoO_2^{2+})$ = rotatory modes of the 8 SO_4^{2-} and 2 MoO_2^{2+} ions, respectively, and N_i (SO_4^{2-}) and $N_i(MoO_2^{2+})$ = internal vibrational modes of the ions, respectively.

Table 9. IR and Raman Bands (in cm^{-1}) and Assignments for $K_2 MoO_2(SO_4)_2$.[a]

IR, powder/KBr Disc at 25 °C	Raman, Crystal at -192 °C	Raman, Crystal at 25 °C	Raman Melt at 430 °C	Tentative Assignments
1286 m	1294, 1273	1291 w		ν_3(str, SO_4^{2-})
1269 m	1266,1253	1265 m	1272 w, dp	ν_3(str, SO_4^{2-})
1198 w	1190 s	1189 s	1172 m, p	ν_3(str, SO_4^{2-})
1154 s	1156 w	1154 w		ν_3(str, SO_4^{2-})
1078 w		1078 vw	1086 w	$K_2S_2O_7$ traces
	1030 s	1026 s	1046 s, p	ν_1(str, SO_4^{2-})
1012 s	1007 w	1007 m		ν_1(str, SO_4^{2-})
976 m	946 vs	943 vs	958 vs, p	$\nu_1(MoO_2^{2+})$
936 s	931 m	928 s		$\nu_3(MoO_2^{2+})$
915 s	919 m	917 s	921 s, dp	$\nu_3(MoO_2^{2+})$
892 s	894 m	892 s		$\nu_1(MoO_2^{2+})$
		822 vw	845 w	
745 w			734 vw	
679 m		676 vw	665 m, p	ν_4(bend, SO_4^{2-})
661w	664 w	662 vw		ν_4(bend, SO_4^{2-})
625 m	628 m	629 m	620 w	ν_4(bend, SO_4^{2-})
613 m	614 w	615 w		ν_4(bend, SO_4^{2-})
594 s	593, 588	596 w	594 w	ν_4(bend, SO_4^{2-})
509 m	514, 510	512 m	540 w	ν_2(bend, SO_4^{2-})
470 m	472 w	471 w	479 vw	ν_2(bend, SO_4^{2-})
450 w,sh	457 w	459 w		ν_2(bend, SO_4^{2-})
	444 w	444 m		ν_2(bend, SO_4^{2-})
	394 s	395 s	392 s, p	$\nu_2(MoO_2^{2+})$
	311 m	308 w	324 w	$\nu_2(MoO_2^{2+})$
	296 m	296 m		$\nu_2(MoO_2^{2+})$
	279 s	280 m	288 m, p	$\nu_2(MoO_2^{2+})$
	254 w	253 w	246 m, p	
	233 s	232 m		
	222, 214			$\nu_{lattice}$
	191 w, 177.5 m			$\nu_{lattice}$
	150, 103, 84,			$\nu_{lattice}$
	78, 61, 36			$\nu_{lattice}$

[a] Intensity codes: w=weak; m=medium; s=strong; sh=shoulder; v=very; p=polarized; dp= depolarized. Calibration: Polystyrene (IR) and Neon (Raman), to a precision of 1 cm^{-1}.

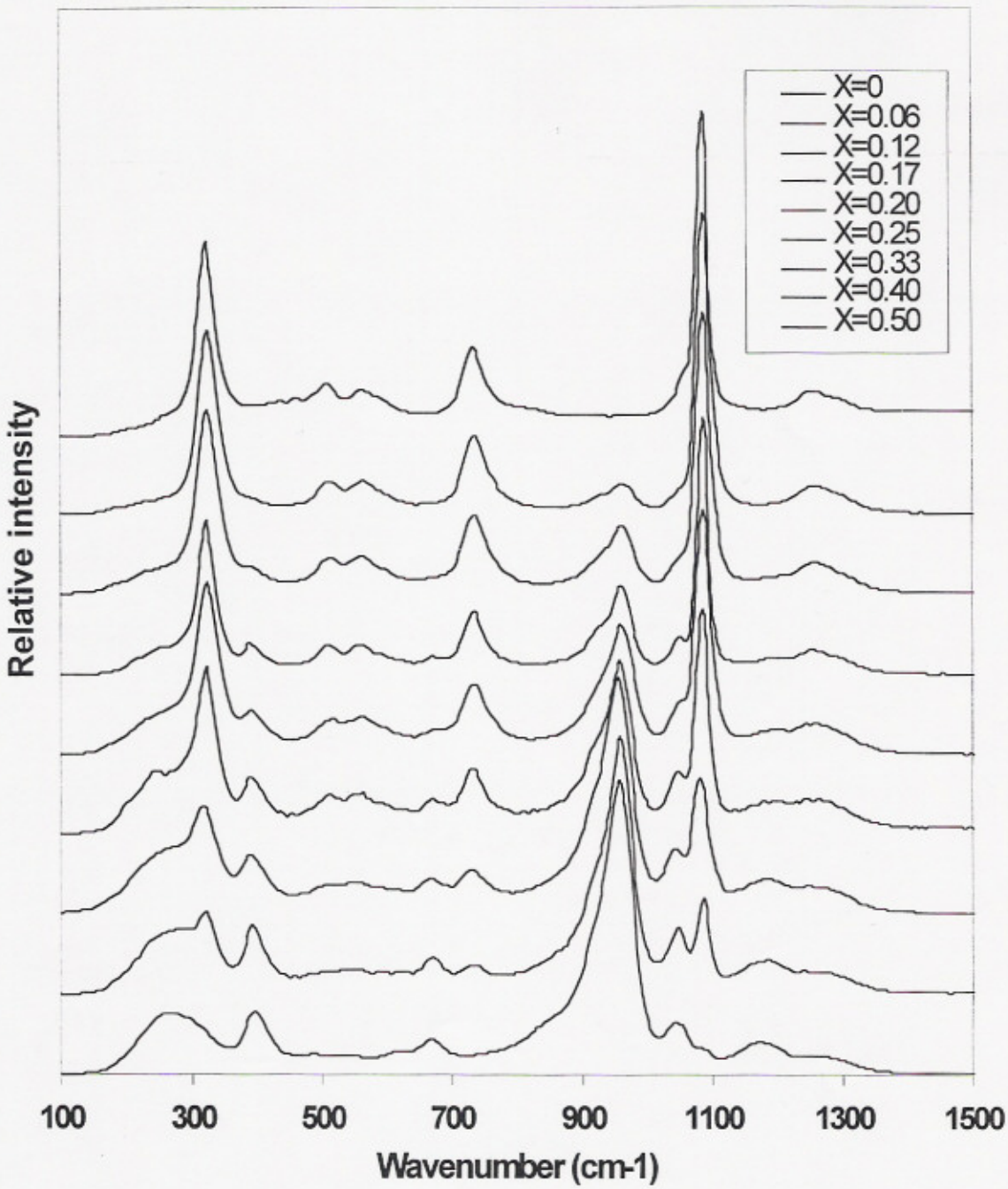

Fig. 1. Raman spectra of melts at 430 °C at different compositions (**X** = formal mole fraction of MoO_3 in the MoO_3 - $K_2S_2O_7$ system). Resolution ca. 10 cm^{-1}.

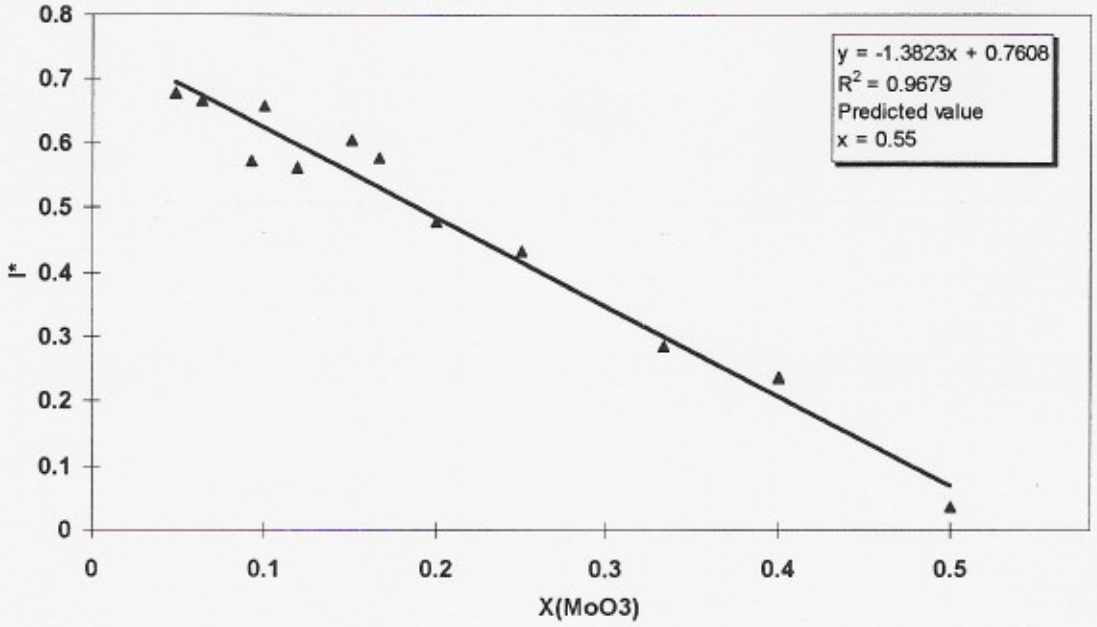

Fig. 2. Plot of the relative Raman intensity ratio I*, as defined in equation 1 *versus* $X(MoO_3)$. A linear regression line is shown, crossing the first axis at 0.55

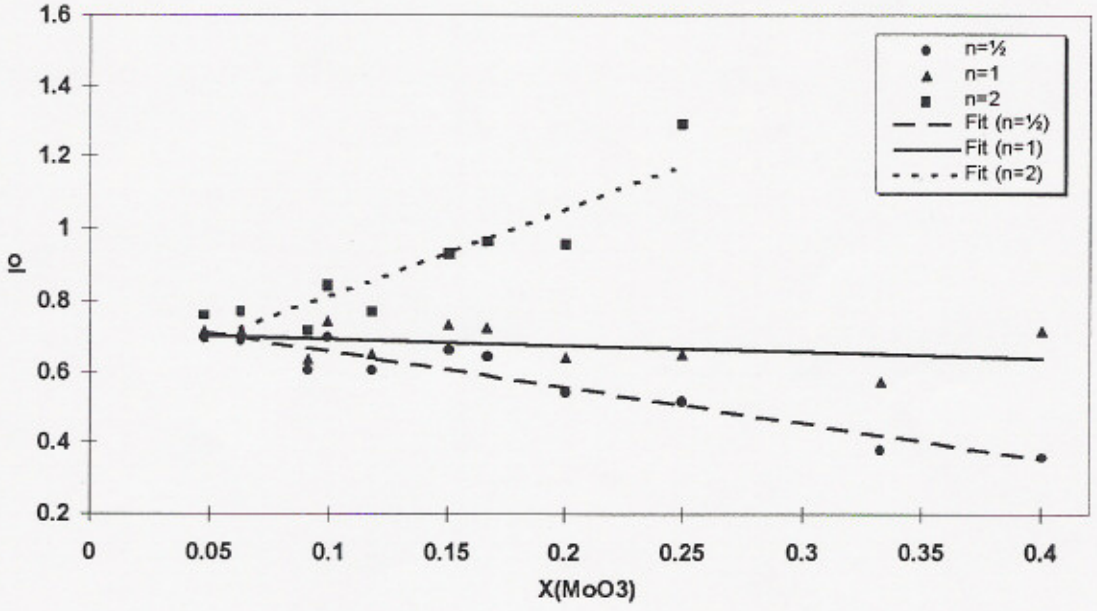

Fig. 3. Plot of the absolute Raman intensity ratio I^O, as defined in equation 2 *versus* $X(MoO_3)$ depending on different assumed *n*-values. Three regression lines are shown. The horisontal line corresponds to the correct *n* value.

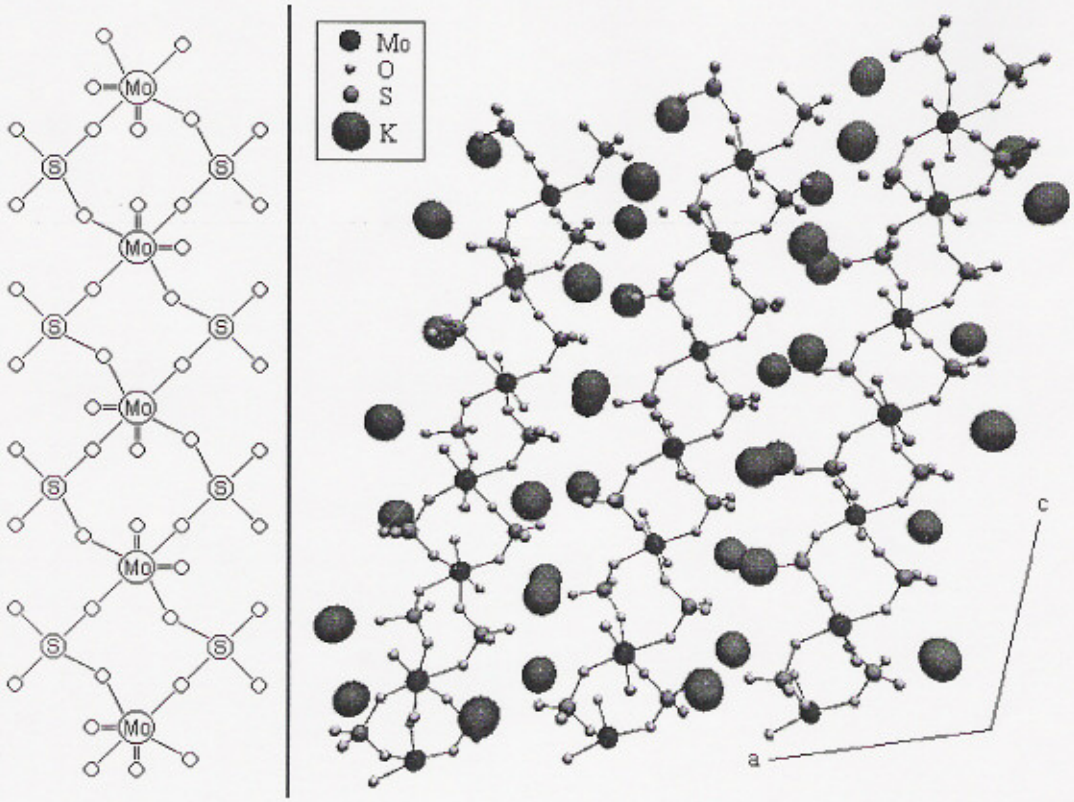

Fig. 4. Projection along the *b*-axis of the structure of $K_2MoO_2(SO_4)_2$. Large K^+ ions are seen between three strands (along the *c*-axis) of sulfato bridged dioxomolybdenum(VI) ions. An idealized drawing of one strand is shown (left). The plot was made using CRYSTINFO (7).

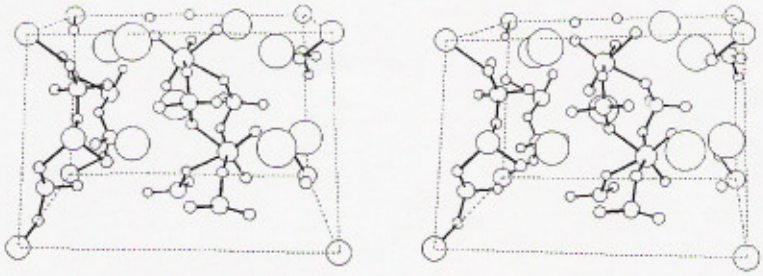

Fig. 5. Stereo plot of the unit cell of $K_2MoO_2(SO_4)_2$, seen along the a-axis.

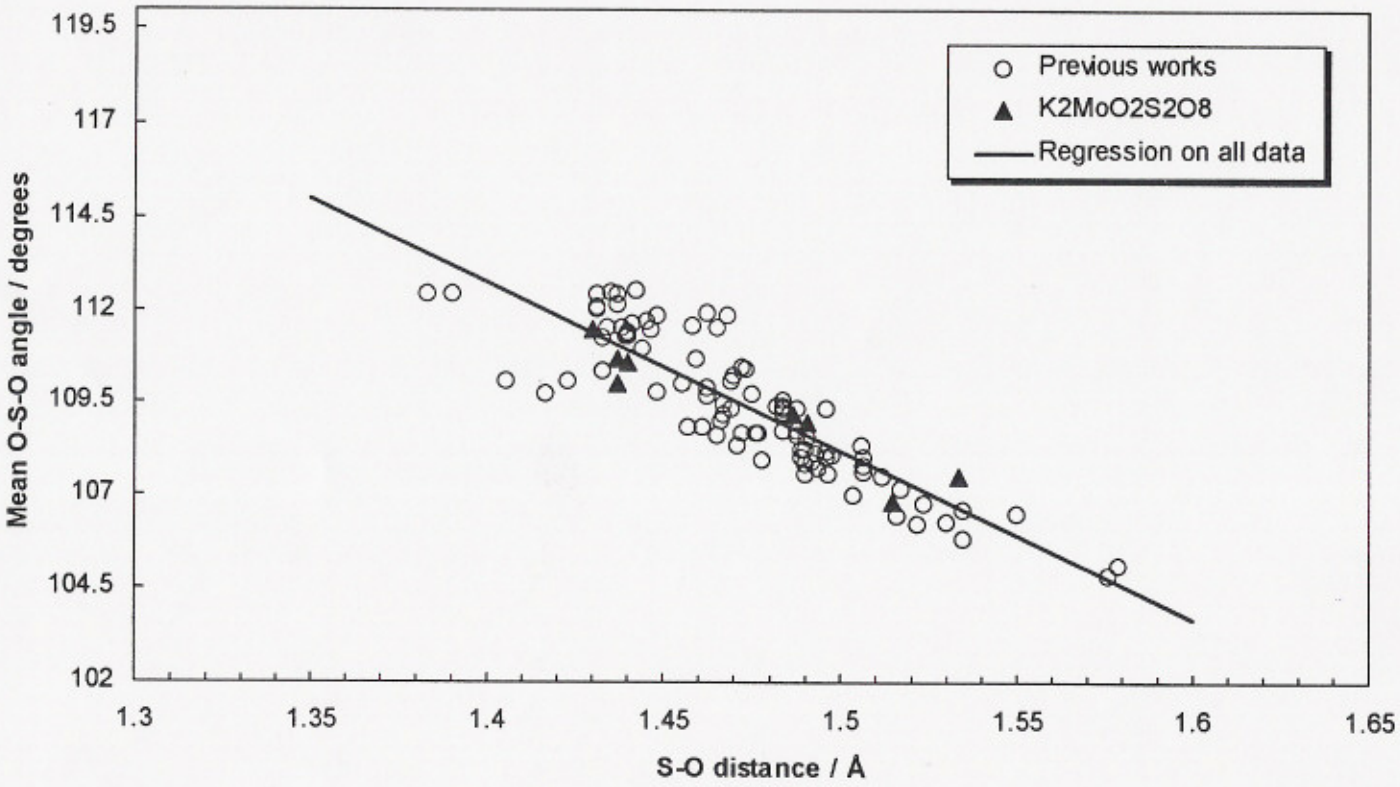

Fig. 6. The distance mean angle relationship of the sulfate tetrahedron. Plot of the average of the three O-S-O angles involving a particular SO bond *versus* its S-O bond distance. Eight solid triangles come from the $K_2MoO_2(SO_4)_2$ structure. Other points are taken from structures of sulfato groups in $KV(SO_4)_2$ (13), $K_4(VO)_3(SO_4)_5$ (14), $Na_2VO(SO_4)_2$ (15), $NaV(SO_4)_2$ (16), $Cs_4(VO)_2(\mu\text{-}O)(SO_4)_4$ (17), $CsV(SO_4)_2$ (18), $Na_3V(SO_4)_3$ (19), β-$VOSO_4$ (20) and $K_6(VO)_4(SO_4)_8$ (21). The regression line was obtained using all points.

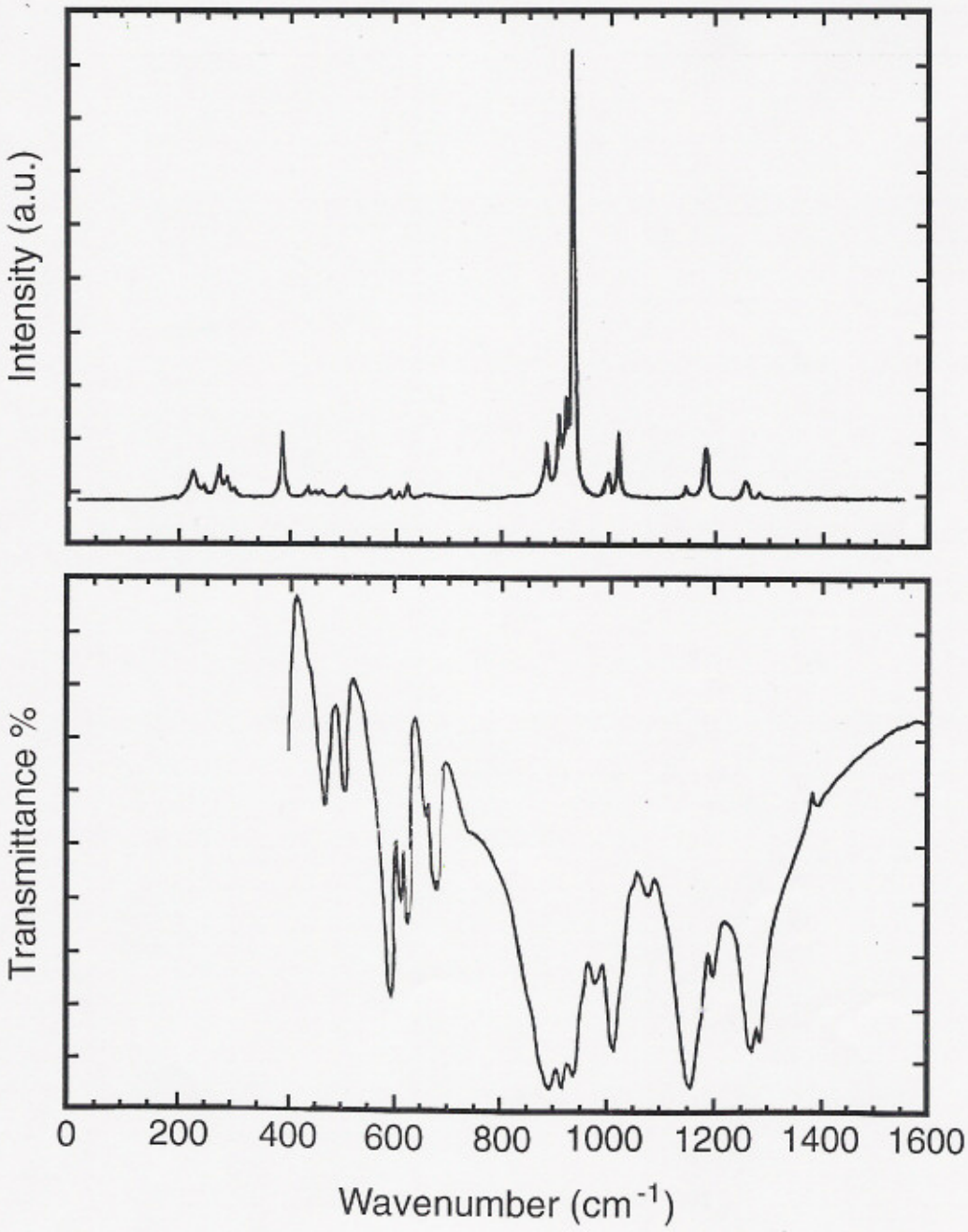

Fig. 7. Raman and IR spectra of $K_2MoO_2(SO_4)_2$ at room temperature. Resolution 4 cm^{-1}.

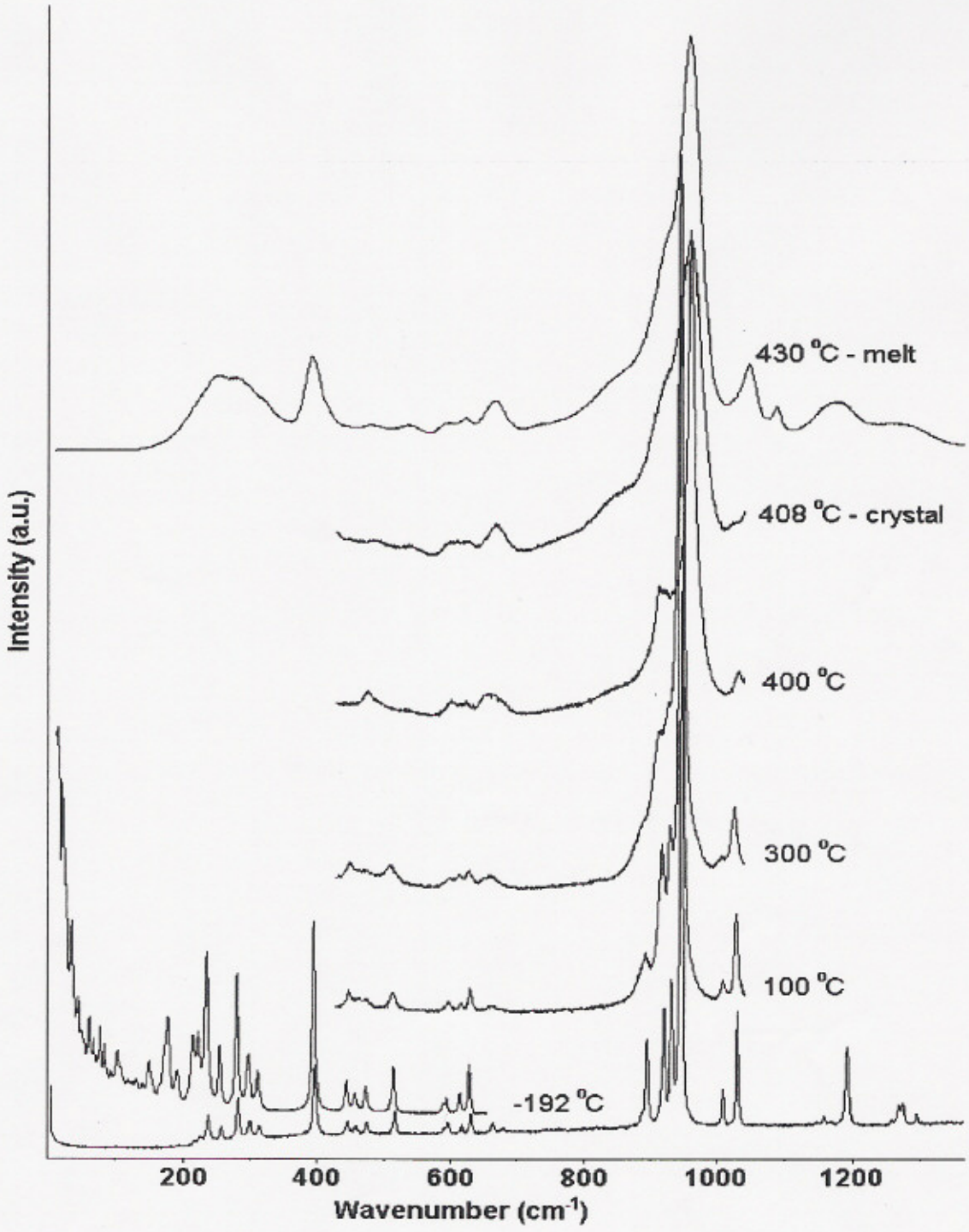

Fig. 8. Raman spectra of crystalline $K_2MoO_2(SO_4)_2$ at different temperatures ranging from -192 °C to the molten state at 430 °C. Resolution 1 cm^{-1}.

THE REACTION BETWEEN MoO_3 AND MOLTEN $K_2S_2O_7$ FORMING $K_2MoO_2(SO_4)_2$, STUDIED BY RAMAN AND IR SPECTROSCOPY AND X-RAY CRYSTAL STRUCTURE DETERMINATION

T. Noerbygaard, R. W. Berg*, and K. Nielsen,
Department of Chemistry, DTU Building 207, Technical University of Denmark,
DK-2800 Lyngby, Denmark

KEY WORDS:

assignment
bridging oxygens
bridging sulfato groups
cis-configuration
bond angles
bonding distances
bond order
bond order sums
bond length
crystal
crystal data
distances
empirical correlations
factor group analysis
Infrared absorption
K^+ ions
$K_2MoO_2(SO_4)_2$,
$K_2S_2O_7$
low temperature
melt
melting point
MoO_2^{2+} ions
MoO_3
MoO_6 octahedra
molybdenum trioxide
octahedral coordination
oxides
oxidation state
potassium pyrosulfate
pyrosulfate
Raman scattering
reaction stoichiometry determination
selection rules
space group
spectroscopy
strands
structure determination
sulfato groups
tentative assignments
trans-influence
vibration
valence
X-ray